NASA/TM—2006-214418

ARL–MR–0644
GT2006–90870

Hybrid Kalman Filter Approach for Aircraft Engine In-Flight Diagnostics: Sensor Fault Detection Case

Takahisa Kobayashi
QSS Group, Inc., Cleveland, Ohio

Donald L. Simon
U.S. Army Research Laboratory, Glenn Research Center, Cleveland, Ohio

October 2006

NASA STI Program . . . in Profile

Since its founding, NASA has been dedicated to the advancement of aeronautics and space science. The NASA Scientific and Technical Information (STI) program plays a key part in helping NASA maintain this important role.

The NASA STI Program operates under the auspices of the Agency Chief Information Officer. It collects, organizes, provides for archiving, and disseminates NASA's STI. The NASA STI program provides access to the NASA Aeronautics and Space Database and its public interface, the NASA Technical Reports Server, thus providing one of the largest collections of aeronautical and space science STI in the world. Results are published in both non-NASA channels and by NASA in the NASA STI Report Series, which includes the following report types:

- TECHNICAL PUBLICATION. Reports of completed research or a major significant phase of research that present the results of NASA programs and include extensive data or theoretical analysis. Includes compilations of significant scientific and technical data and information deemed to be of continuing reference value. NASA counterpart of peer-reviewed formal professional papers but has less stringent limitations on manuscript length and extent of graphic presentations.

- TECHNICAL MEMORANDUM. Scientific and technical findings that are preliminary or of specialized interest, e.g., quick release reports, working papers, and bibliographies that contain minimal annotation. Does not contain extensive analysis.

- CONTRACTOR REPORT. Scientific and technical findings by NASA-sponsored contractors and grantees.

- CONFERENCE PUBLICATION. Collected papers from scientific and technical conferences, symposia, seminars, or other meetings sponsored or cosponsored by NASA.

- SPECIAL PUBLICATION. Scientific, technical, or historical information from NASA programs, projects, and missions, often concerned with subjects having substantial public interest.

- TECHNICAL TRANSLATION. English-language translations of foreign scientific and technical material pertinent to NASA's mission.

Specialized services also include creating custom thesauri, building customized databases, organizing and publishing research results.

For more information about the NASA STI program, see the following:

- Access the NASA STI program home page at *http://www.sti.nasa.gov*

- E-mail your question via the Internet to *help@sti.nasa.gov*

- Fax your question to the NASA STI Help Desk at 301–621–0134

- Telephone the NASA STI Help Desk at 301–621–0390

- Write to:
  NASA STI Help Desk
  NASA Center for AeroSpace Information
  7121 Standard Drive
  Hanover, MD 21076–1320

NASA/TM—2006-214418

ARL–MR–0644
GT2006–90870

Hybrid Kalman Filter Approach for Aircraft Engine In-Flight Diagnostics: Sensor Fault Detection Case

Takahisa Kobayashi
QSS Group, Inc., Cleveland, Ohio

Donald L. Simon
U.S. Army Research Laboratory, Glenn Research Center, Cleveland, Ohio

Prepared for
Turbo Expo 2006
sponsored by the American Society of Mechanical Engineers
Barcelona, Spain, May 8–11, 2006

National Aeronautics and
Space Administration

Glenn Research Center
Cleveland, Ohio 44135

October 2006

Acknowledgments

This research was funded by the NASA Aviation Safety and Security Program as a task under the Propulsion System Safety Technologies Element.

Level of Review: This material has been technically reviewed by technical management.

Available from

NASA Center for Aerospace Information
7121 Standard Drive
Hanover, MD 21076–1320

National Technical Information Service
5285 Port Royal Road
Springfield, VA 22161

Available electronically at http://gltrs.grc.nasa.gov

Hybrid Kalman Filter Approach for Aircraft Engine In-Flight Diagnostics: Sensor Fault Detection Case

Takahisa Kobayashi
QSS Group, Inc.
Cleveland, Ohio 44135

Donald L. Simon
U.S. Army Research Laboratory
Glenn Research Center
Cleveland, Ohio 44135

Abstract

In this paper, a diagnostic system based on a uniquely structured Kalman filter is developed for its application to in-flight fault detection of aircraft engine sensors. The Kalman filter is a hybrid of a nonlinear on-board engine model (OBEM) and piecewise linear models. The utilization of the nonlinear OBEM allows the reference health baseline of the diagnostic system to be updated, through a relatively simple process, to the health condition of degraded engines. Through this health baseline update, the diagnostic effectiveness of the in-flight sensor fault detection system is maintained as the health of the engine degrades over time. The performance of the sensor fault detection system is evaluated in a simulation environment at several operating conditions during the cruise phase of flight.

Introduction

In-flight diagnostics of aircraft gas turbine engines is a critical task for the improvement of aviation safety. The capability to detect and/or isolate any faults, which may cause the engine to operate at an undesirable condition during flight, can improve not only the safety but also the efficiency of engine operation. Since the diagnostic system results can influence the follow-on actions taken by the flight crew or control system, it is critical that they be highly reliable. In-flight diagnostic systems, therefore, must be designed with robustness to non-fault-related factors which exist in the real environment and can potentially mislead diagnostic systems to generate incorrect results.

In-flight diagnostic systems are, in general, designed at a nominal health, or non-degraded, condition. This design condition becomes a reference health baseline for the diagnostics; any observed deviation in engine outputs from their reference condition values indicates the presence of a fault. In-flight diagnostic systems can perform effectively as long as the health of a real engine remains in the vicinity of the reference health baseline, thereby making engine output deviations prominent when a fault takes place.

As the real engine degrades over time, in-flight diagnostic systems may lose their effectiveness. Engine health degradation is a normal aging process that occurs to all aircraft engines due to usage, and therefore is not considered as a fault. However, similar to various faults, degradation causes the engine outputs to deviate from their reference condition values. When engine output deviations eventually exceed a certain level, the diagnostic systems may misinterpret the health degradation as a fault and consequently generate a false alarm.

One approach to maintaining the effectiveness of in-flight diagnostics applied to degraded engines is to periodically update or re-design the diagnostic algorithms based on the estimated amount of health degradation. Health degradation can be estimated by trend monitoring systems using post-flight data (refs. 1 to 3). Through the update based on the estimated health degradation, the health baseline of an in-flight diagnostic system can be shifted to the vicinity of the degraded engine, and therefore the system is able to effectively detect the presence of a fault. One issue with this approach is its practicality. Depending on the complexity of the diagnostic algorithms, the update process may take too much time and thus may be impractical.

To address the above issue, a Kalman filter based in-flight sensor fault detection system is developed in this paper. The proposed Kalman filter is composed of a nonlinear on-board engine model (OBEM) and piecewise linear state-space models, which include Kalman gain matrices. With this architecture, the system update to account for engine health degradation is achieved through a relatively simple process: by feeding the estimated health degradation values into the OBEM. Thus, fault detection can be accomplished even without updating linear models and associated Kalman gains as the real engine degrades over time.

In the following sections of this paper, the problem setup and the design approach for an in-flight sensor fault detection system are descried, followed by the application of the design methodology to a large commercial aircraft engine model. To validate its diagnostic effectiveness, the in-flight sensor fault detection system is evaluated in a simulation environment using various fault and degradation scenarios at multiple operating conditions during the cruise phase of flight.

Nomenclature

BST	Booster
CGEKF	Constant Gain Extended Kalman Filter
HPC	High Pressure Compressor
HPT	High Pressure Turbine
LPT	Low Pressure Turbine
OBEM	On-Board Engine Model
P2	Engine inlet pressure
P25	HPC inlet pressure
P_{amb}	Ambient pressure
PLA	Power Lever Angle

PLKF	Piecewise Linear Kalman Filter
PS3	Combustor inlet static pressure
T2	Engine inlet temperature
T3	Combustor inlet temperature
T49	LPT inlet temperature
T_{amb}	Ambient temperature
TMHS23	BST metal temperature
TMHS3	HPC metal temperature
TMHS41	HPT nozzle metal temperature
TMHS42	HPT metal temperature
TMHS5	LPT metal temperature
TMSHBC	Combustor case metal temperature
TMHSBL	Combustor liner metal temperature
VBV	Variable bleed valve
VSV	Variable stator vane
WF36	Fuel flow
WSSR	Weighted Sum of Squared Residuals
XN12	Fan speed, measured
XN25	Core speed, measured
XNH	Core speed, actual
XNL	Fan speed, actual
e	Environmental parameter vector
h	Health parameter vector
h_{ref}	Reference health condition vector
u_{cmd}	Control command vector
v	Sensor noise vector
x	State variable vector
y	Sensor output vector (controls/diagnostics)
z	Sensor output vector (ambient/engine inlet)

Problem Setup for an In-Flight Fault Detection System

The objective of an in-flight fault detection system is to detect faults as quickly as possible from the observed engine outputs while avoiding false alarms and missed detections. Since false alarms are generated as the result of misinterpretation of non-fault-related factors, it is important to understand the influence of such factors on engine outputs. Engine health degradation is one of the non-fault-related factors that can cause false alarms. As shown in figure 1, engine health degradation is described as gradual deviations of health parameters from the initial healthy baseline. Health parameters are efficiencies and flow capacities of engine components such as compressors and turbines, and they indicate the health of such components. As they deviate from the initial healthy baseline, engine outputs will also deviate from their nominal condition values. Since degradation is a normal aging process that all aircraft engines will experience due to usage, it is not considered a fault, whereas a fault is an abnormal and unexpected event. However, as the engine output deviations increase with time due to the progression of health degradation, it becomes difficult to distinguish the presence of faults from health degradation through the observation of engine outputs. As a result, an in-flight fault detection system loses its diagnostic effectiveness as the engine degrades over time. An example of such loss of diagnostic effectiveness, due to health gradation, is shown in references 4 and 5 for the case of sensor fault diagnostics based on Neural Networks.

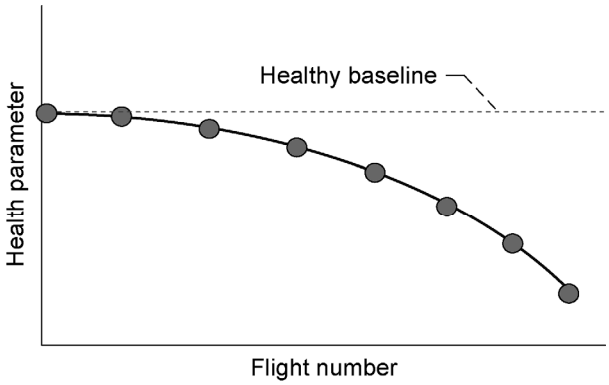

Figure 1.—Engine health degradation.

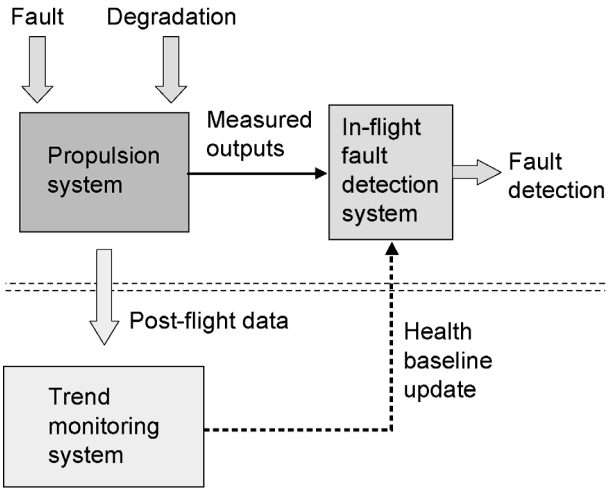

Figure 2.—Process of health baseline update.

To reduce the influence of health degradation on in-flight diagnostic performance, the fault detection system needs to be updated periodically based on the estimated amount of health degradation, as shown in figure 2. Health degradation can be estimated by trend monitoring systems using post-flight data (refs. 1 to 3). Since health degradation progresses gradually with time, it is expected that the actual change in health parameters is small for a number of flights. Therefore, the process of estimating health degradation and updating the in-flight diagnostic system needs to be accomplished once per a number of flights. When the updating process is complete, the estimated health condition becomes the new reference baseline for the fault detection system, as shown in figure 3, until the next update process is completed. Through this periodic baseline update, the in-flight diagnostic system can operate in the vicinity of the degraded engine and thus maintain its effectiveness for fault detection.

In this paper, it is assumed that a trend monitoring system, which is capable of estimating engine health degradation (health parameters), is available. Moreover, it is assumed that

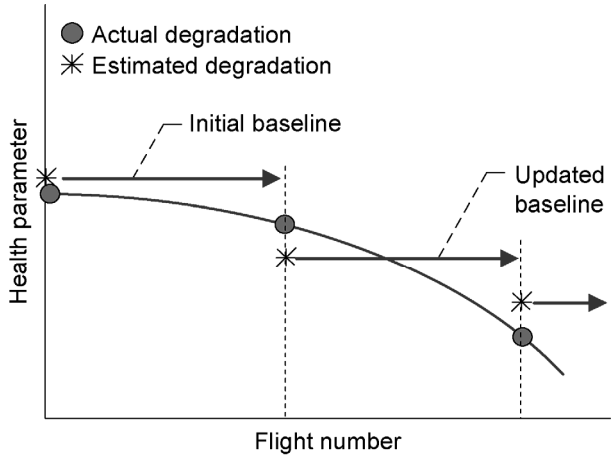

Figure 3.—Baseline update using estimated health degradation.

this trend monitoring system will achieve a certain level of precision in its estimation performance. The rest of the paper focuses on the development of the in-flight sensor fault detection system based on the hybrid Kalman filter approach.

Development of an In-Flight Sensor Fault Detection System

The in-flight fault detection system described in this section is based on the Kalman filter approach with a unique hybrid architecture. The Kalman filter is composed of a nonlinear on-board engine model (OBEM) and piecewise linear state-space models, which include Kalman gain matrices. The OBEM is a physics-based model designed to run in real time, while the piecewise linear state-space models are derived off-line from the OBEM at the nominal health baseline. These two main components are merged together to form the "hybrid" Kalman filter. Based on the residuals generated by the hybrid Kalman filter, a fault indicator signal is constructed for detecting faults.

Hybrid Kalman Filter Design

The design steps for the hybrid Kalman filter are exactly the same as those for the general linear Kalman filter. First, a nonlinear plant model is linearized at operating points. Then, Kalman gains are computed based on the linear representations of the plant model. When implemented, however, linear models and associated Kalman gains are integrated with the nonlinear plant model. An aircraft engine under consideration is represented by a nonlinear model of the following form:

$$\begin{aligned} \dot{x} &= f(x, h, u_{cmd}, e) \\ y &= g(x, h, u_{cmd}, e) + v \end{aligned} \tag{1}$$

where x, h, u_{cmd}, and e represent the vectors of state variables, health parameters, control command inputs, and environmental parameters, respectively. For given input values, the nonlinear functions f and g generate the vectors of state derivatives $\dot{x}$ and sensor outputs y. The sensor outputs are corrupted by the white noise vector v. By linearizing the engine model at a reference health baseline (e.g., nominal health condition) and also at a specific environmental condition, the following state-space equations are obtained:

$$\begin{aligned} \dot{x} &= A(x - x_{ss}) + B(u_{cmd} - u_{ss}) + L(h - h_{ref}) \\ y - y_{ss} &= C(x - x_{ss}) + D(u_{cmd} - u_{ss}) + M(h - h_{ref}) + v \end{aligned} \tag{2}$$

where A, B, C, D, L, and M are the state-space matrices with appropriate dimensions. The vectors x_{ss}, y_{ss}, u_{ss} contain the steady-state values at which the engine model is trimmed for linearization. The vector h_{ref} represents a reference health baseline. The Kalman gain is computed based on the matrix pair [A, C], and the linear Kalman filter equation is given as follows:

$$\begin{aligned} \dot{\hat{x}} &= A(\hat{x} - x_{ss}) + B(u_{cmd} - u_{ss}) + K(y - \hat{y}) \\ \hat{y} - y_{ss} &= C(\hat{x} - x_{ss}) + D(u_{cmd} - u_{ss}) \end{aligned} \tag{3}$$

The vectors $\hat{x}$ and $\hat{y}$ represent the estimates of the state variables and sensor outputs, respectively. The matrix K represents the Kalman gain. In order for the Kalman gain to converge, the matrix pair [A, C] must be observable.

It should be noted that the linear Kalman filter in equation (3) does not account for the influence of health parameter deviations from the reference health baseline in equation (2). Since the Kalman filter is designed with some robustness to system uncertainty in the form of process noise, it has robustness to health parameter deviations to some extent. However, the Kalman filter does not have the level of robustness that can handle the full health deterioration that an engine will experience over its lifetime. Therefore, as discussed in references 6 and 7, the Kalman filter must be updated periodically based on the estimated health condition in order to allow the Kalman filter to operate in the vicinity of a real engine as it degrades. The process of health baseline update for the general linear Kalman filter is described in the following four steps: 1) estimate the health degradation, 2) trim the closed-loop engine model at the new reference health baseline (estimated health condition), which should be close to the actual health condition, and generate the steady-state vectors, 3) linearize the open-loop engine model and generate state-space matrices, and then 4) compute the Kalman gain. Step 1 can be done off-line by a trend monitoring system which monitors the engine health degradation over time. Steps 3 and 4 may not be necessary according to reference 6, but step 2 alone can be a time-consuming, troublesome process, especially when many operating points must be covered over the flight envelope. Thus, it is desirable to simplify the update process in order to make it feasible in the real application environment.

Insight on simplifying the health baseline update process can be found from past studies. Reference 6 indicated that the

performance of the linear Kalman filter when applied to degraded engines can be improved significantly just by updating the steady-state vectors (x_{ss}, y_{ss}, u_{ss}) to the new values derived at degraded conditions. Moreover, reference 8 demonstrated that the constant gain extended Kalman filter can operate over a wide operating range despite its simple architecture, which basically combines a nonlinear engine model with a single Kalman gain matrix computed at a single operating point. These studies indicate that the Kalman gain itself is not of primary importance to operate the Kalman filter in the environment where various elements, such as health or flight condition, are changing. Rather, the accuracy of the plant model is of primary importance.

Based on the above knowledge, the hybrid Kalman filter is developed by replacing the steady-state vectors of equation (3) with the following nonlinear OBEM:

$$\begin{aligned} \dot{x}_{OBEM} &= f\left(x_{OBEM}, \hat{h}_{ref}, u_{cmd}, z\right) \\ y_{OBEM} &= g\left(x_{OBEM}, \hat{h}_{ref}, u_{cmd}, z\right) \end{aligned} \tag{4}$$

where the vector $\hat{h}_{ref}$ represents the health condition estimated by a trend monitoring system, which is updated once per a number of flights. The vector z represents the measured parameters which define the flight condition. By integrating the OBEM and linear state-space models, the following hybrid Kalman filter is formed:

$$\begin{aligned} \dot{\hat{x}} &= A\left(\hat{x} - x_{OBEM}\right) + K\left(y - \hat{y}\right) \\ \hat{y} &= C\left(\hat{x} - x_{OBEM}\right) + y_{OBEM} \end{aligned} \tag{5}$$

In equation (5), the steady-state vectors which appeared in equation (3) were replaced by the state variables and engine outputs generated by the OBEM. Furthermore, the control command inputs and associated matrices B and D in equation (3) do not appear in equation (5) since the effect of control command inputs is accounted for by the OBEM as seen in equation (4).

There are a few things which should be noted about the hybrid structure. First, the hybrid Kalman filter depends on the OBEM but not vice versa. The OBEM runs in parallel with the actual engine at the estimated health condition without receiving any feedback signals from the hybrid Kalman filter. Therefore, the numerical stability of the OBEM is not influenced by the performance of the hybrid Kalman filter. The objective of the OBEM is to generate the state variables and sensor outputs at the estimated health condition. By updating the health condition of the OBEM, its state variables and sensor outputs can be brought close to the values of the degraded engine. Since health condition mismatches still exist between the OBEM and the degraded engine due to estimation errors, sensor output mismatches also exist between them. The objective of the hybrid Kalman filter, or specifically its linear component, is to further improve the sensor output matching between its estimates and the measured values through the tuning of the state variable estimates. As long as the OBEM operates in the vicinity of the degraded engine (i.e., health condition estimation errors are small), the hybrid Kalman filter will maintain its accurate sensor output estimation performance.

Construction of Fault Indicator Signal

The validation of the Kalman filter estimates is generally done by checking residuals, or the differences between the measured and estimated sensor output values. If residuals are large, it can be considered that the Kalman filter is generating inaccurate sensor output estimates because of the presence of an anomaly, such as a sensor fault, that was not accounted for in the Kalman filter design. To indicate the presence of a fault, a weighted sum of squared residuals (WSSR) is computed as follows:

$$WSSR = \left(y - \hat{y}\right)^T \Sigma^{-1} \left(y - \hat{y}\right) \tag{6}$$

where

$$\Sigma = diag\left[\sigma^2\right]$$

The vector σ represents the standard deviation of the sensor measurements. The square matrix Σ normalizes the residual vector $\left(y - \hat{y}\right)$. Since the hybrid Kalman filter design discussed in the previous section does not account for the presence of a sensor fault, the value of the fault indicator signal, WSSR, should increase when such a fault occurs in the system. The next step for detecting a fault is to compare the fault indicator signal to a pre-established detection threshold. When the fault indicator signal exceeds the detection threshold, it is considered that a fault indeed exists in the system. The establishment of a detection threshold can be based on statistics or achieved through systematic analysis.

Overall Architecture of the In-Flight Sensor Fault Detection System

The overall architecture of the in-flight sensor fault detection system is shown in figure 4. The fault detection system receives the measured variables (y and z) and control

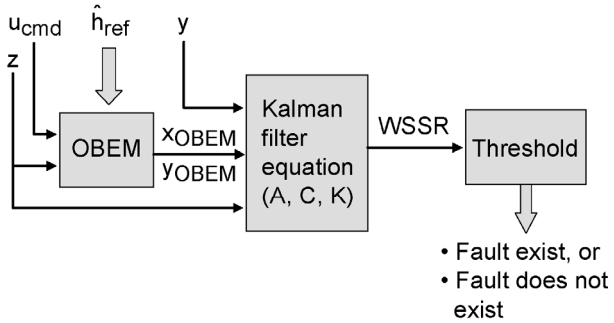

Figure 4.—Overall architecture of the in-flight fault detection system.

commands (u_{cmd}) from the on-board digital engine control unit, while receiving a periodically updated health baseline ($\hat{h}_{ref}$) from the trend monitoring system. The output of the fault detection system is one of two possibilities: fault exists or fault does not exist. The fault detection system reveals only the existence of a fault, not its identity or severity.

Since the current system is designed without any restrictions on the types of faults it should detect, it may detect faults in something other than sensors. Additional faults that an engine may encounter during flight include actuator and component faults. Similar to the case of sensor faults, actuator and component faults must be detected through the observation of sensor output deviations. However, the level of sensor output deviations due to these faults heavily depends on location of sensors. Some of the actuator and component faults, therefore, may be very difficult to detect with a given set of sensors unless their fault magnitude is significantly large. Although it is desirable to detect any type of fault, the focus of the current system is placed on sensor fault detection.

Fault detection is the first step in the diagnostic process. It only reveals the existence of a fault without identifying the nature of the detected fault. After fault detection comes fault isolation (refs. 6 and 7) and then fault accommodation (refs. 9 and 10).

Application of the Hybrid Kalman Filter Methodology to Aircraft Engine Model

In this section, the in-flight sensor fault detection system based on the hybrid Kalman filter is applied to an aircraft engine model. A description of the engine model is given first, followed by a discussion of the piecewise linear models. Then, the derivation of the fault detection threshold is discussed.

Engine Model

The engine model used in this paper is a nonlinear simulation of an advanced high-bypass turbofan engine, a typical power plant for a large commercial aircraft. This engine model has been constructed as a Component Level Model (CLM), which consists of the major components of an aircraft engine. The CLM represents highly complex engine physics while designed to run in real time. Engine performance deviations from the nominal health baseline are modeled by adjustments to efficiency and flow capacity scalars of the following five components: Fan (FAN), Booster (BST), High-Pressure Compressor (HPC), High-Pressure Turbine (HPT), and Low-Pressure Turbine (LPT). There are a total of 10 of these adjustments which are called health parameters. The engine state variables, health parameters, actuator variables, and environmental parameters are shown in table 1.

TABLE 1.—STATE VARIABLES, HEALTH PARAMETERS, ACTUATORS, AND ENVIRONMENTAL PARAMETERS

State variables	XNL, XNH, TMHS23, TMHS3 TMHSBL, TMHSBC, TMHS41 TMHS42, TMHS5
Health parameters	FAN efficiency, FAN flow capacity BST efficiency, BST flow capacity HPC efficiency, HPC flow capacity HPT efficiency, HPT flow capacity LPT efficiency, LPT flow capacity
Actuators	WF36, VBV, VSV
Environmental parameters	Altitude, Mach number Ambient temperature

There are a total of 11 measured parameters (y and z in figure 4) that are available to the digital engine control unit of this engine. Table 2 shows seven sensors (y) along with their standard deviations given in percent of steady-state values at the ground maximum power condition. The control actions and diagnostics are based on those sensed variables. Table 3 shows four additional measured parameters (z) along with their standard deviations given in their actual units. These four parameters indicate the ambient and engine inlet conditions. Some of them (T_{amb}, P_{amb}, and T2) are equivalent to the environmental parameters in table 1, while T2 and P2 are used for parameter corrections (ref. 11).

TABLE 2.—STANDARD DEVIATIONS OF CONTROLS AND DIAGNOSTICS SENSORS (σ IN PERCENT OF STEADY-STATE VALUES AT GROUND MAXIMUM POWER CONDITION)

Sensors (y)	σ (%)
XN12	0.25
XN25	0.25
P25	0.50
T25	0.75
PS3	0.50
T3	0.75
T49	0.75

TABLE 3.—STANDARD DEVIATIONS OF AMBIENT AND ENGINE INLET SENSORS (σ IN ACTUAL UNITS)

Sensors (z)	σ
T_{amb}	5.0 °F
P_{amb}	0.1 psi
T2	5.0 °F
P2	0.1 psi

This nonlinear engine model is used to represent both the actual engine and the OBEM in the subsequent sections. Typically, there will be a mismatch between the model and the actual engine due to modeling errors and un-modeled elements. The influence of such a mismatch will be assessed in the later section. The engine model representing an actual engine operates at given health conditions, and its flight condition is specified by the three environmental parameters in table 1. The OBEM operates at estimated health conditions, and its flight condition is specified by three measured parameters: T_{amb}, P_{amb}, and T2. The actual engine and the OBEM receive the same three control commands (table 1). In the current control architecture, the power lever angle (PLA) is converted to desired corrected fan speed (an indicator of thrust). The control system adjusts three actuation values to cause the corrected measured fan speed to match the desired value. The closed-loop engine simulation runs with a 0.02-second time step.

Piecewise Linear Model Design

The linear component of the hybrid Kalman filter (A, C, K in equation (5)) is designed using the nonlinear engine model through the following steps. The nonlinear engine model is first linearized at specific operating conditions. For each of the linear engine models, a Kalman gain is computed. Then, the piecewise linear models are saved in table lookup form. As the operating condition moves from one point to another, the piecewise linear models are interpolated based on a scheduling parameter as discussed in reference 7.

The unique aspect of the hybrid Kalman filter design is that the piecewise linear models are integrated with the OBEM, instead of the steady-state vectors for the case of a pure piecewise linear Kalman filter design (refs. 7 and 12). As discussed earlier, having an accurate plant representation is of primary importance in the Kalman filter operation. Because of the usage of the OBEM, which is a good representation of an actual engine, the number of operating conditions at which the piecewise linear models are derived does not have to be as many as the case for a pure piecewise linear Kalman filter design. In this paper, the piecewise linear models are generated along the steady-state power setting line at a cruise condition. For the interpolation of the piecewise linear models, the corrected fan speed (XN12) is used as the scheduling parameter. A preliminary study indicated that this specific hybrid Kalman filter design maintains its accurate estimation performance over a wide operating range. When a similar study was done for the hybrid Kalman filter using piecewise linear models generated at sea level static condition, the estimation performance was not as good as the case of cruise condition design. Better estimation performance may be achieved by linking linear models generated at multiple flight conditions, such as climb and cruise. However, it is desirable to keep the number of piecewise linear models as small as possible, since a lesser number of linear models reduces design complexity and also improves execution speed.

When the hybrid Kalman filter was implemented in a simulation environment, the system was discretized to run at the frequency of 50 Hz. The parameters used by the hybrid Kalman filter algorithm are corrected based on the engine inlet condition T2 and P2.

Selection of the Detection Threshold

The selection of the detection threshold is a critical part in the diagnostic system design. Setting the threshold at a low value increases the chance of detecting faults but also increases the chance of generating false alarms. Conversely, setting the threshold at a high value decreases the chance of generating false alarms but also decreases the chance of detecting faults. As such, the balance between true positive (fault detection) and false positive (false alarms) is adjusted by the threshold. It is statistically impossible to achieve zero false alarm rates while detecting any faults, but it is the general consensus that the false alarm rate should be maintained as low as possible. Keeping that in mind, the threshold is determined in this section.

A false alarm is the result of misinterpretation of non-fault-related factors[1] which exist in various forms to various degrees. If the influence of such factors on the fault indicator signal is known, a threshold can be derived from that knowledge. Among the numerous non-fault-related factors that can cause false alarms, health condition mismatches are used as an example to derive the threshold.

As discussed earlier, in the current approach, the health baseline of the OBEM must be updated periodically as the health of the real engine degrades gradually with time. However, the health baseline update will never be exact in the real environment, and therefore, health condition mismatches will always exist between the OBEM and the real engine. These mismatches can cause the fault indicator signal (WSSR in equation (6)) to increase. If the threshold is set to a point higher than the maximum value that the fault indicator signal can reach due to health condition mismatches, then false alarms can be avoided at least for the case of health condition mismatches.

To investigate the influence of health condition mismatches on the fault indicator signal, 300 cases of health degradation and associated health condition estimates were first generated. Three hundred cases of health degradation were created by randomly shifting all 10 health parameters shown in table 1. The deviation values were uniformly distributed over the range from 1 to 5 percent, and this level of deviation is beyond the typical level of engine-to-engine variation due to manufacturing tolerance. Estimated health conditions were created by adding estimation errors to the 300 cases of health degradation. The estimation error for each health parameter was a random number with uniform distribution over the range of ±0.5 percent. As mentioned earlier, it is assumed that a trend monitoring system is available, and its estimation accuracy is assumed to be within ±0.5 percent from the actual values.

[1]Engine health degradation is one of these factors, but its contribution to the cause of false alarms is reduced through the health baseline update. Other examples of non-fault-related factors are customer bleeds, horsepower extractions, and dirt washout from fan and compressors.

Using the above 300 health condition mismatch cases, the engine and the hybrid Kalman filter were run for 100 seconds at a specific operating point. For each mismatch case, the hybrid Kalman filter generated a time history of the fault indicator signal. Then, the maximum value that the fault indicator signal reached during the 100-second run was saved for each of the 300 cases. Based on the maximum WSSR values for the 300 cases, a histogram was generated to investigate the variation of the fault indicator signal due to health condition mismatches. This process was then repeated at various flight conditions with various power settings. Examples of the histograms generated at three power settings (PLA = 65, 69, and 70) at a cruise condition are shown in figure 5. In the current implementation, the fault indicator signal (WSSR) has been scaled and also processed by a low pass filter with a cutoff frequency of 0.1 rad/sec. The arrows in the figure indicate the largest maximum WSSR value among the 300 cases.

From the histograms generated at various operating conditions, it was found that the largest maximum WSSR value generally increases and becomes an outlier in the distribution as the power setting increases. This tendency can be seen in figure 5. After extensive study, it was found that this is due to the fact that health condition mismatches (as large as ±0.5 percent) can on rare occasions result in quite large mismatches in the state variables and sensor outputs between the engine and the OBEM at high power settings. Under the presence of such large mismatches in sensor outputs, the hybrid Kalman filter performs poorly since its linear component can improve the sensor output matching only to a limited extent.

From the above observation, it would be a reasonable approach to use different threshold values at different power settings in order to achieve effective fault detection performance. The threshold selection in this section is focused on the cruise condition where the power setting is in the intermediate range. At high power settings, such as takeoff and climb, different thresholds must be determined.

As can be seen in figure 5, the largest maximum WSSR value becomes a noticeable outlier in the distribution around 70° PLA. Similar tendencies were also observed at different flight conditions. Since the nominal power setting is in the range of 60 to 65° PLA during cruise phase, the threshold is set to the value of 1.60. With this threshold value, some margin is available at 65° PLA. This threshold value is used for the PLA value up to 69°. To further ensure that the threshold violation is due to the existence of a fault, the persistency of threshold violation is checked before declaring the fault. It was determined that the threshold must be violated 25 consecutive time steps (0.5 second) to declare fault detection. The threshold value and persistency test are adjusted based on the engineering judgment of the designer, and the performance of the fault detection system will vary with those design factors. In the following section, the performance of the fault detection system is evaluated using the threshold value of 1.60.

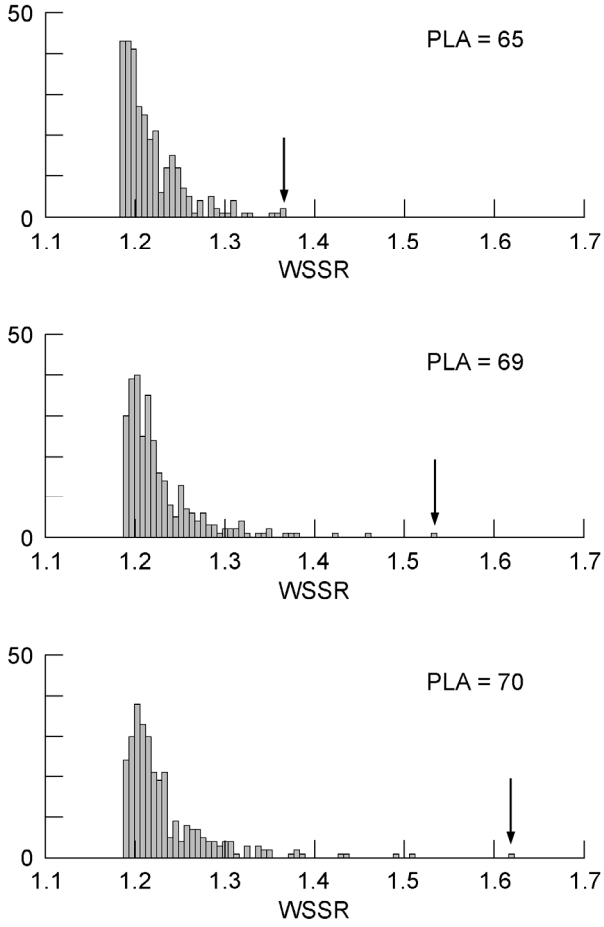

Figure 5.—Histograms of maximum WSSR values for 300 health condition mismatch cases at cruise.

Performance Evaluation

In this section, the sensor fault detection system is evaluated at a cruise condition. First, the minimum bias that the system can detect for individual sensors is determined at two power settings (PLA = 65 and 69) with three different health condition cases. Then, the fault detection system is evaluated to determine if it would generate a false alarm during transient operations by running the engine simulation model through moderate transient scenarios.

Sensor Bias Detection

The value of the detection threshold determined in the previous section was based on the 300 cases of health condition mismatch between the engine and the OBEM. With this threshold value, no false alarm is generated at least for those 300 cases of health condition mismatch. As discussed earlier, decreasing the chance of generating false alarms also decreases the chance of detecting faults. Thus, to evaluate the suitability of the threshold value, the minimum bias that can be detected for individual sensors is determined in this section.

If the level of detectable sensor bias is not acceptable, the threshold value must be adjusted accordingly.

The minimum detectable bias is determined for individual sensors by running the engine simulation and the hybrid Kalman filter for 100 seconds at a steady-state cruise condition. When the fault indicator signal (WSSR) exceeds the detection threshold for 25 consecutive time steps, a fault is detected.

Table 4 shows the minimum bias detected for each sensor at 65° PLA at three different health conditions. The bias values are given in terms of measurement standard deviations. For the nominal health case, both the engine and the OBEM are set to the nominal health condition. This case represents an ideal scenario where no health mismatches exist between the engine and the OBEM. For degradation case A, the engine and the OBEM are set to degraded and estimated health conditions, respectively. This case represents a more realistic scenario where health condition mismatches exist. As can be seen in figure 5, health condition mismatches cause the WSSR value to vary. The health condition used in case A is the one whose WSSR value represents the 90th percentile value in the 65° PLA histogram of figure 5; the WSSR values of 270 cases (90 percent) are less than or equal to the WSSR value at the health condition used in case A. Degradation case B is similar to case A, except that the health condition used in case B results in the largest WSSR value among the 300 cases.

TABLE 4.—MINIMUM DETECTABLE SENSOR BIAS AT 65° PLA (NUMBERS IN TERMS OF STANDARD DEVIATIONS)

	Nominal health	Degradation A	Degradation B
XN12	6.4/–6.4	6.9/–4.6	7.4/–3.2
XN25	5.4/–5.4	5.4/–3.9	6.4/–3.0
P25	1.9/–1.9	1.6/–1.8	1.3/–1.6
T25	2.9/–2.9	2.2/–2.8	1.7/–3.3
PS3	2.4/–2.4	1.4/–3.2	0.9/–3.7
T3	3.7/–3.7	3.0/–3.8	2.3/–3.4
T49	4.4/–4.5	4.0/–4.0	3.6/–3.2
T_{amb}	0.4/–0.5	0.3/–0.5	0.2/–0.6
P_{amb}	0.7/–0.6	0.8/–0.5	0.8/–0.3
T2	0.6/–0.6	0.7/–0.4	0.7/–0.3
P2	----------	----------	----------

From table 4, it can be observed that, for the nominal health case, the bias magnitudes that can be detected are symmetric between the positive and negative directions. Such symmetry, however, does not appear in degradation cases A and B where the health condition mismatches exist. The health condition mismatches result in sensor output mismatches between the engine and the OBEM. Consequently, the WSSR value increases and gets closer to the detection threshold as seen in figure 5. Therefore, a smaller magnitude bias, when compared to the nominal health case, can be detected if a bias and the corresponding sensor's output mismatch are in the same direction (positive or negative). On the other hand, if a bias is in the opposite direction of the corresponding sensor's output mismatch, the bias counteracts the sensor output mismatch to some extent, and thus it requires a larger magnitude to be detected. From table 4, it can be observed that the skewness between the positive and negative biases is more prominent in degradation case B than case A.

Table 4 also shows that very small biases are detected for those sensors which indicate the ambient and engine inlet conditions. At first glance, these numbers may lead one to conclude that the fault detection system is too sensitive to biases in those sensors. The reason for such sensitivity is that three sensors (T_{amb}, P_{amb}, and T2) define the flight condition for the OBEM and thus a bias in these sensors causes the OBEM to operate at a different flight condition. Since altitude and Mach number can be calculated from those three measurements, it may be necessary to compare the calculated values to measured altitude and Mach number in order to validate those three sensors. The fault detection system was not able to detect a bias in the P2 sensor. This sensor is currently used for the correction of pressure measurements. Since both measured and estimated pressure values are corrected by the P2 value, a bias in this sensor does not increase the residuals.

Table 5 shows the minimum bias detected for each sensor at 69° PLA at three different health conditions. This example is similar to the previous case except that the power setting is higher, and thus health condition mismatches can results in the WSSR value closer to the detection threshold. For the nominal health case, both the engine and the OBEM are set to the nominal health condition. For degradation cases C and D, the engine and the OBEM are set to degraded and estimated health conditions, respectively. The health condition mismatch of case C results in the 90th percentile WSSR value in the 69° PLA histogram of figure 5, whereas that of case D results in the largest WSSR value among the 300 cases.

TABLE 5.—MINIMUM DETECTABLE SENSOR BIAS AT 69° PLA (NUMBERS IN TERMS OF STANDARD DEVIATIONS)

	Nominal health	Degradation C	Degradation D
XN12	6.0/–5.9	6.0/–4.5	1.0/–10.4
XN25	5.9/–6.0	5.5/–4.4	1.1/–7.0
P25	1.9/–1.9	1.6/–1.8	2.6/–0.3
T25	3.0/–2.9	2.7/–2.7	3.3/–0.9
PS3	2.3/–2.3	1.5/–2.7	2.5/–0.4
T3	3.5/–3.5	2.5/–3.8	2.8/–0.8
T49	4.2/–4.2	3.2/–4.3	2.1/–1.6
T_{amb}	0.4/–0.4	0.4/–0.5	0.6/–0.1
P_{amb}	0.7/–0.6	0.7/–0.6	0.1/–1.0
T2	0.6/–0.6	0.7/–0.5	0.1/–0.8
P2	----------	----------	----------

At the nominal health condition, the fault detection system appears to perform in a consistent manner; the level of detectable bias at this power setting is similar to that of the previous case of the 65° PLA, and the detectable bias magnitudes are symmetric between the positive and negative directions. The above observation, however, does not hold for degradation cases C and D. Especially for degradation case D where the WSSR value gets very close to the detection threshold, the level of skewness between the positive and

negative directions is very prominent. For some of the sensors, smaller magnitude biases, when compared to the nominal health case, can be detected in both positive and negative directions. This gives an impression that it is advantageous to have health condition mismatches so that smaller magnitude biases can be detected. It should be understood, however, that the closer the WSSR gets to the detection threshold due to health condition mismatches, the higher the chance of generating false alarms becomes. From tables 4 and 5, it is obvious that health condition mismatches and power settings have significant influence on the level of detectable sensor biases. The reader should be reminded that these results show the level of bias that will trigger a fault detection alarm. The detection algorithm will not identify the biased sensor; it only indicates that a fault exists.

Minor Transient Operation for False Alarm Test

The detection threshold used in this paper has been fixed to a specific value for its application during cruise phase. The fixed threshold seems to be applicable as long as the engine operates under steady-state conditions. Since it is desirable to extend the operation of the fault detection system to transient cases, the applicability of the fixed threshold is evaluated in this section by running the engine simulation through minor transient operations. If minor transient operation causes the WSSR value to exceed the fixed threshold, an adaptive threshold, whose value changes as the engine undergoes transients, must be used as was done in reference 13 in order to avoid false alarms.

For this evaluation, the engine and the hybrid Kalman filter are run under the following six transient scenarios:

1) PLA is ramped from 60 to 69° in 1 second. After steady-state operation, PLA is ramped back to 60° in 1 second.
2) In addition to the PLA ramp in scenario 1, altitude is increased by 1000 ft in 10 seconds. After steady-state operation, altitude is decreased by 1000 ft in 10 seconds.
3) In addition to the PLA ramp in scenario 1, Mach number is increased by 0.02 in 5 seconds. After steady-state operation, Mach number is decreased by 0.02 in 5 seconds.
4) Same as scenario 1 except that a turbine clearance model is added to the engine model.
5) Same as scenario 2 except that a turbine clearance model is added to the engine model.
6) Same as scenario 3 except that a turbine clearance model is added to the engine model.

Each transient scenario is 200 seconds long, and the time histories of three inputs (PLA, altitude, Mach number) are shown in figure 6. Scenarios 4 through 6 are a repeat of scenarios 1 through 3 except that a turbine clearance model is added to the engine model. Since it is unlikely that the real engine is perfectly modeled in the OBEM, there will be model mismatch, other than health condition mismatches, between the real engine and the OBEM. In scenarios 4 through 6, a turbine clearance model, which represents the turbine clearance dynamics with high fidelity, is added only to the

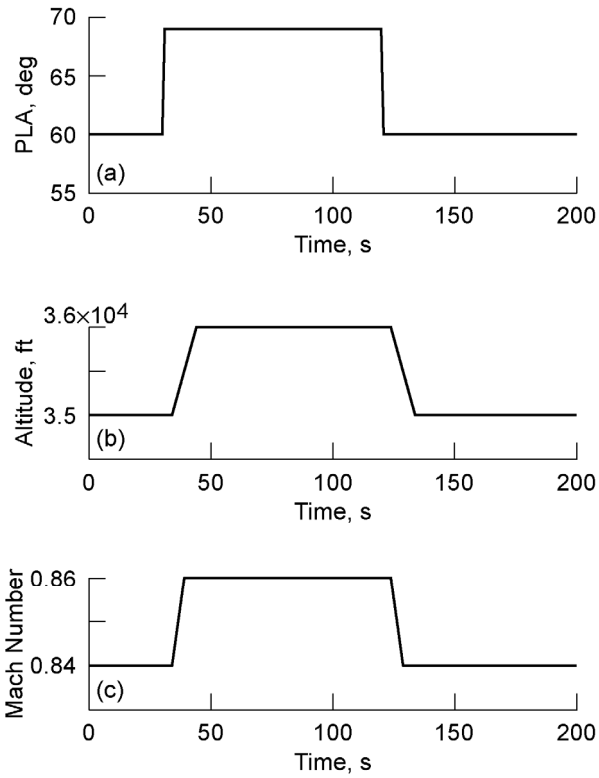

Figure 6.—Time history of transient inputs. (a) Input for scenarios 1 through 6. (b) Input for scenarios 2 and 5. (c) Input for scenarios 3 and 6.

engine model representing a real engine in order to introduce unknown dynamics. The presence of the turbine clearance model introduces sensor output mismatches between the engine and the OBEM during transient operations.

The engine simulation and the hybrid Kalman filter were run through the six transient scenarios at five health conditions: nominal health and degradation levels used in cases A through D in tables 4 and 5. Table 6 shows the result of this simulation test. The symbol "O" indicates that no false alarm was generated, "X" indicates that a false alarm was generated. Figure 7 shows the time histories of the WSSR for transient scenario 2 at the nominal health (solid line) and degradation D (dashed line).

TABLE 6.—FALSE ALARM TEST WITH MINOR TRANSIENT SCENARIOS (O: NO FALSE ALARM, X: FALSE ALARM)

		Transient scenario					
		1	2	3	4	5	6
Health condition	Nominal	O	O	O	O	O	O
	Degr. A	O	O	O	O	O	O
	Degr. B	O	O	O	O	O	O
	Degr. C	O	O	O	O	O	O
	Degr. D	O	X	O	O	X	O

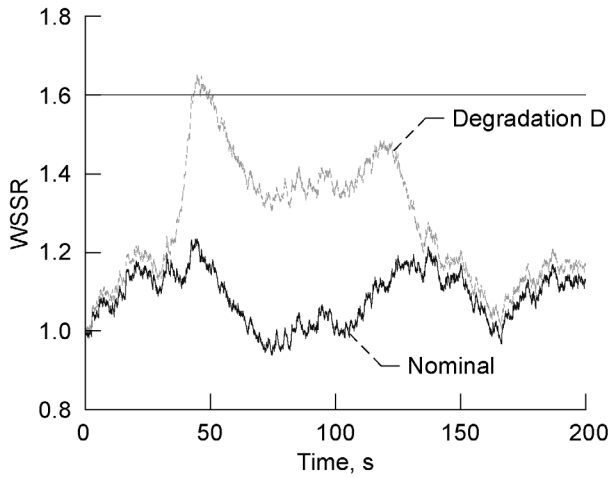

Figure 7.—WSSR responses for transient scenario 2.

As was noted in figure 5, the WSSR gets very close to the detection threshold at degradation case D with 69° PLA. The minor transient of scenario 2, in which both PLA and altitude are ramped, causes the WSSR to exceed the threshold temporarily but long enough (at least 25 consecutive time steps) to generate a false alarm. In order to avoid false alarms, the threshold value or the period of persistency check must be adjusted as the engine undergoes transient operations.

Another observation made during the transient test is that the turbine clearance model caused an increase in the sensor output mismatch between the engine and the OBEM at the nominal health and degradation case D. However, in other degradation cases, the turbine clearance model caused a reduction in the sensor output mismatch. Similar to some of the sensor bias cases, it appears that the turbine clearance model counteracted health condition mismatch, resulting in better sensor output matching between the engine and the OBEM. Thus, the presence of unknown dynamics in the engine does not mean that the estimation performance of the Kalman filter always gets worse.

Discussion

The unique structure of the hybrid Kalman filter possesses advantages over conventional Kalman filter approaches and is well suited for application to in-flight diagnostics. In this section, some benefits of the hybrid architecture are discussed.

One obvious benefit of the hybrid architecture is that the reference health baseline of the hybrid Kalman filter can be updated to the health condition of the degraded engine in a relatively simple manner: by feeding the estimated health condition values to the OBEM. This update process is much simpler than for the case of the pure piecewise linear Kalman filter (PLKF) approach. Without the baseline update, the fault detection system loses its diagnostic effectiveness as the real engine degrades over time. To evaluate the significance of the baseline update, the hybrid Kalman filter was applied to the 300 degraded engines, used in the previous sections, without going through the health baseline update. When the reference baseline of the hybrid Kalman filter was fixed to the nominal health condition, the fault detection system misinterpreted degradation as a fault in 283 engines out of 300 (94.3 percent false alarm rate). Obviously, such a high false alarm rate is not acceptable, and thus the baseline update is a necessary step.

Another benefit is that the hybrid Kalman filter combines the advantages of the constant gain extended Kalman filter (CGEKF) approach (refs. 8 and 14) and the PLKF approach (ref. 7). The advantage of the CGEKF over the PLKF is its capability to capture the nonlinearity of engine operation under the influence of faults. For instance, when an engine experiences a fault, the control system adjusts the actuator positions to meet its objective, such as maintaining fan speed at the commanded value. Because of such control adjustments, the engine moves to a new operating condition which may be a significant deviation from the condition before the fault occurrence. Such nonlinear engine operation due to closed-loop control effects in the presence of fault can be captured by the CGEKF and the hybrid Kalman filter but not by the PLKF. Although the CGEKF approach has such an advantage over the PLKF approach, it also has disadvantages in other areas. As noted in reference 14, the numerical stability of the CGEKF may not be as robust as that of the PLKF. Since the nonlinear engine model of the CGEKF receives feedback signals (residuals multiplied by a Kalman gain matrix), large residuals may drive the nonlinear engine model out of the range that the model was designed for. If this happens even for a short period, the numerical stability of the CGEKF may be lost. On the other hand, in the hybrid Kalman filter approach, the numerical stability of the nonlinear engine model is not influenced by the estimation process since the OBEM does not receive any feedback signals. The OBEM runs as a stand-alone engine simulation, generating state variables and sensor outputs at a given health baseline. Based on the information provided by the OBEM, the Kalman filter algorithm is processed using the piecewise linear state-space models. As such, the hybrid Kalman filter possesses the numerical stability of the PLKF approach and also the nonlinear estimation capability of the CGEKF approach.

Finally, the hybrid Kalman filter approach can be easily expanded to a bank of Kalman filters for its application to fault isolation (refs. 6 and 7). In the hybrid architecture, only the linear component of the filter (A, C, K) must be expanded while keeping only one OBEM. By combining one OBEM and multiple piecewise linear models, each of which is designed based on a unique fault hypothesis, a bank of hybrid Kalman filters can be formed. Therefore, this level of expansion is similar to the case of the pure PLKF approach.

Conclusion

The hybrid Kalman filter approach was developed for its application to in-flight sensor fault detection. The hybrid Kalman filter has a unique architecture which is composed of a nonlinear on-board engine model (OBEM) and piecewise linear state-space models. In this hybrid architecture, the OBEM functions as an integral part between the off-line and real-time diagnostic systems; it operates at a reference health

baseline specified by a trend monitoring system and provides information needed to process the Kalman filter algorithm for in-flight diagnostics. Because of this integration, the in-flight sensor fault detection system does not need to deal with engine health degradation by itself.

To validate this approach, the in-flight sensor fault detection system was evaluated in a simulation environment using a nonlinear model of a large commercial aircraft engine. Its performance was evaluated at multiple steady-state operating points at a cruise condition and also evaluated over minor transients. The performance of the sensor fault detection system was satisfactory in general; however, further study is needed in some areas to improve its capability. It was found that a fixed threshold is not good enough to cover the range of operation that an engine may undergo during flight. For some cases of health condition mismatch between the engine and the OBEM, the value of the fault indicator signal became large at high power settings. In order to avoid false alarms, the threshold must be adjusted according to the power setting and also adjusted during transients. Therefore, the utilization of an adaptive threshold is needed to improve the overall capability of the in-flight sensor fault detection system.

References

1. Doel, D.L., 1994, "TEMPER—A Gas Path Analysis Tool for Commercial Jet Engines," Journal of Engineering for Gas Turbines and Power, 116, pp. 82–89.
2. Volponi, A.J., 1994, "Sensor Error Compensation in Engine Performance Diagnostics," ASME Paper 94–GT–58.
3. Kobayashi, T., and Simon, D.L., 2005, "Hybrid Neural-Network Genetic-Algorithm Technique for Aircraft Engine Performance Diagnostics," Journal of Propulsion and Power, 21, pp. 751–758.
4. Mathioudakis, K., and Romessis, C., 2004, "Probabilistic Neural Networks for Validation of On-Board Jet Engine Data," Proceedings of the Institution of Mechanical Engineers, Part G: Journal of Aerospace Engineering, 218, pp. 59–72.
5. Romessis, C., and Mathioudakis, K., 2003, "Setting Up of a Probabilistic Neural Network for Sensor Fault Detection Including Operation With Component Faults," Journal of Engineering for Gas Turbines and Power, 125, pp. 634–641.
6. Kobayashi, T., and Simon, D.L., 2003, "Application of a Bank of Kalman Filters for Aircraft Engine Fault Diagnostics," ASME Paper GT2003–38550.
7. Kobayashi, T., and Simon, D.L., 2005, "Evaluation of an Enhanced Bank of Kalman Filters for In-Flight Aircraft Engine Sensor Fault Diagnostics," Journal of Engineering for Gas Turbines and Power, 127, pp. 497–504.
8. Kobayashi, T., Simon, D.L., and Litt, J.S., 2005, "Application of a Constant Gain Extended Kalman Filter for In-Flight Estimation of Aircraft Engine Performance Parameters," ASME Paper GT2005–68494.
9. Rausch, R., Viassolo, D.E., Kumar, A., Goebel, K., Eklund, N., Brunell, B., and Bonanni, P., 2004, "Towards In-Flight Detection and Accommodation of Faults in Aircraft Engines," AIAA Paper 2004–6463.
10. Rausch, R.T., Goebel, K.F., Eklund, N.H., and Brunell, B.J., 2005, "Integrated In-Flight Fault Detection and Accommodation: A Model-Based Study," ASME Paper GT2005–68300.
11. Volponi, A.J., 1999, "Gas Turbine Parameter Corrections," Journal of Engineering for Gas Turbines and Power, 121, pp. 613–621.
12. Luppold, R.H., Roman, J.R., Gallops, G.W., and Kerr, L.J., 1989, "Estimating In-Flight Engine Performance Variations Using Kalman Filter Concepts," AIAA Paper AIAA–89–2584.
13. Merrill, W.C., DeLaat, J.C., and Bruton, W.M., 1988, "Advanced Detection, Isolation, and Accommodation of Sensor Failures—Real-Time Evaluation," Journal of Guidance, Control, and Dynamics, 11, pp. 517–526.
14. Sugiyama, N., 2000, "System Identification of Jet Engines," Journal of Engineering for Gas Turbines and Power, 122, pp. 19–26.

REPORT DOCUMENTATION PAGE

Form Approved
OMB No. 0704-0188

1. AGENCY USE ONLY (*Leave blank*)	2. REPORT DATE	3. REPORT TYPE AND DATES COVERED
	October 2006	Technical Memorandum

4. TITLE AND SUBTITLE

Hybrid Kalman Filter Approach for Aircraft Engine In-Flight Diagnostics: Sensor Fault Detection Case

5. FUNDING NUMBERS

WBS 645846.02.07.03

6. AUTHOR(S)

Takahisa Kobayashi and Donald L. Simon

7. PERFORMING ORGANIZATION NAME(S) AND ADDRESS(ES)

National Aeronautics and Space Administration
John H. Glenn Research Center at Lewis Field
Cleveland, Ohio 44135–3191

8. PERFORMING ORGANIZATION REPORT NUMBER

E–15698

9. SPONSORING/MONITORING AGENCY NAME(S) AND ADDRESS(ES)

National Aeronautics and Space Administration
Washington, DC 20546–0001
and
U.S. Army Research Laboratory
Adelphi, Maryland 20783–1145

10. SPONSORING/MONITORING AGENCY REPORT NUMBER

NASA TM—2006-214418
ARL–MR–0644
GT2006–90870

11. SUPPLEMENTARY NOTES

Prepared for Turbo Expo 2006 sponsored by the American Society of Mechanical Engineers, Barcelona, Spain, May 8–11, 2006. Takahisa Kobayashi, QSS Group, Inc., 21000 Brookpark Road, Cleveland, Ohio 44135; and Donald L. Simon, U.S. Army Research Laboratory, NASA Glenn Research Center. Responsible person, Donald L. Simon, organization code RIC, 216–433–3740.

12a. DISTRIBUTION/AVAILABILITY STATEMENT

Unclassified - Unlimited
Subject Category: 07

Available electronically at http://gltrs.grc.nasa.gov

This publication is available from the NASA Center for AeroSpace Information, 301–621–0390.

12b. DISTRIBUTION CODE

13. ABSTRACT ***(Maximum 200 words)***

In this paper, a diagnostic system based on a uniquely structured Kalman filter is developed for its application to in-flight fault detection of aircraft engine sensors. The Kalman filter is a hybrid of a nonlinear on-board engine model (OBEM) and piecewise linear models. The utilization of the nonlinear OBEM allows the reference health baseline of the diagnostic system to be updated, through a relatively simple process, to the health condition of degraded engines. Through this health baseline update, the diagnostic effectiveness of the in-flight sensor fault detection system is maintained as the health of the engine degrades over time. The performance of the sensor fault detection system is evaluated in a simulation environment at several operating conditions during the cruise phase of flight.

14. SUBJECT TERMS

Aircraft engines; Fault detection; Kalman filter; On-board engine model; In-flight fault detection, Flight safety

15. NUMBER OF PAGES

17

16. PRICE CODE

17. SECURITY CLASSIFICATION OF REPORT	18. SECURITY CLASSIFICATION OF THIS PAGE	19. SECURITY CLASSIFICATION OF ABSTRACT	20. LIMITATION OF ABSTRACT
Unclassified	Unclassified	Unclassified	